The Canadian Mineralogist
Vol. 35, pp. 119-133 (1997)

MANGANOAN-FAYALITE-BEARING GRANITIC PEGMATITE FROM QUIRRA, SARDINIA: RELATION TO HOST PLUTONIC ROCKS AND TECTONIC AFFILIATION

ELISABETTA PANI

C.N.R., Centro Studi Geominerari e Mineralurgici, c/o DIGITA, Università di Cagliari, Piazza d'Armi, 09123 Cagliari, Italy

ROBERTO RIZZO

Dipartimento di Geoingegneria e Tecnologie Ambientali, Università di Cagliari, Piazza d'Armi, 09123 Cagliari, Italy

MATI RAUDSEPP

Department of Earth and Ocean Sciences, 6339 Stores Road, The University of British Columbia, Vancouver, British Columbia V6T 1Z4

Abstract

Manganoan-fayalite-bearing pegmatites occur at the northern margin of the Mt. Perdosu granitic pluton in the Quirra region, southeast Sardinia, Italy, in the apical part of a more extensive granitic complex. The granitic massif comprises post-orogenic A-type subsolvus biotite and biotite–muscovite leucogranites and minor monzogranites of the aluminous trend, emplaced at a shallow depth at the end of the Hercynian orogeny. In the study area, pegmatites occur as lenses, veinlets, and pockets. All of the pegmatites are hosted in granitic rocks close to their contact with metamorphic rocks, and are characterized by locally abundant altered and unaltered manganoan fayalite, together with quartz and alkali feldspar. Fayalite occurs as partly altered large crystals up to several tens of cm in size, as smaller, severely altered crystalline aggregates, and as micrometer-scale, largely unaltered drop-like inclusions in quartz. Generally, the altered crystals of fayalite are enclosed in alkali feldspar, against which rims of biotite, chlorite and magnetite have developed. Subhedral to euhedral magnetite, manganoan grunerite, greenalite, ferripyrophyllite and laihunite are the products of subsolidus alteration of the fayalite. On the basis of geological, mineralogical and geochemical data, these pegmatites are considered to be products of crystallization of a residual liquid from a parent magma, the composition of which can be represented by the least evolved granitic rocks outcropping in the area.

Keywords: granitic pegmatite, manganoan fayalite, A-type granite, Sardinia, Italy.

Sommaire

Nous décrivons des exemples de pegmatite granitique à fayalite près de la bordure nord du pluton granitique du mont Perdosu, dans la région de Quirra, du sud-est de la Sardaigne, en Italie. Il s'agit de la partie apicale d'un complexe granitique plus étendu. Le massif granitique est fait de leucogranites post-orogéniques subsolvus de type A, à biotite ou à biotite + muscovite, et de venues monzogranitiques mineures, le tout définissant une lignée hyperalumineuse; ces roches ont été mises en place à faible profondeur au terme de l'orogenèse hercynienne. Dans la région étudiée, les pegmatites se présentent sous forme de lentilles, de veinules, et de poches, toutes encaissées dans des roches granitiques près du contact avec des roches métamorphiques. Dans chaque cas, la pegmatite contient de la fayalite manganifère, localement abondante et altérée, avec quartz et feldspath alcalin. La fayalite se présente en gros cristaux atteignant plusieurs dizaines de centimètres de taille, tous partiellement altérés, en agrégats plus petits, dont l'altération est plus avancée, et en "goutelettes" généralement non altérées dans le quartz. En général, les cristaux altérés sont encaissés dans le feldspath alcalin, le long duquel on peut voir un liseré de biotite, chlorite et magnétite. Un assemblage de magnétite sub-idiomorphe à idiomorphe, grunerite manganifère, greenalite, ferripyrophyllite et laïhunite résulte de l'altération subsolidus de la fayalite. A la lumière des données géologiques, minéralogiques et géochimiques, ces pegmatites représenteraient des produits de cristallisation d'un liquide résiduel issu d'un magma parental dont la composition peut être représentée par les granites les moins évolués qui affleurent dans cette région.

(Traduit par la Rédaction)

Mots-clés: pegmatite granitique, fayalite manganifère, granite de type A, Sardaigne, Italie.

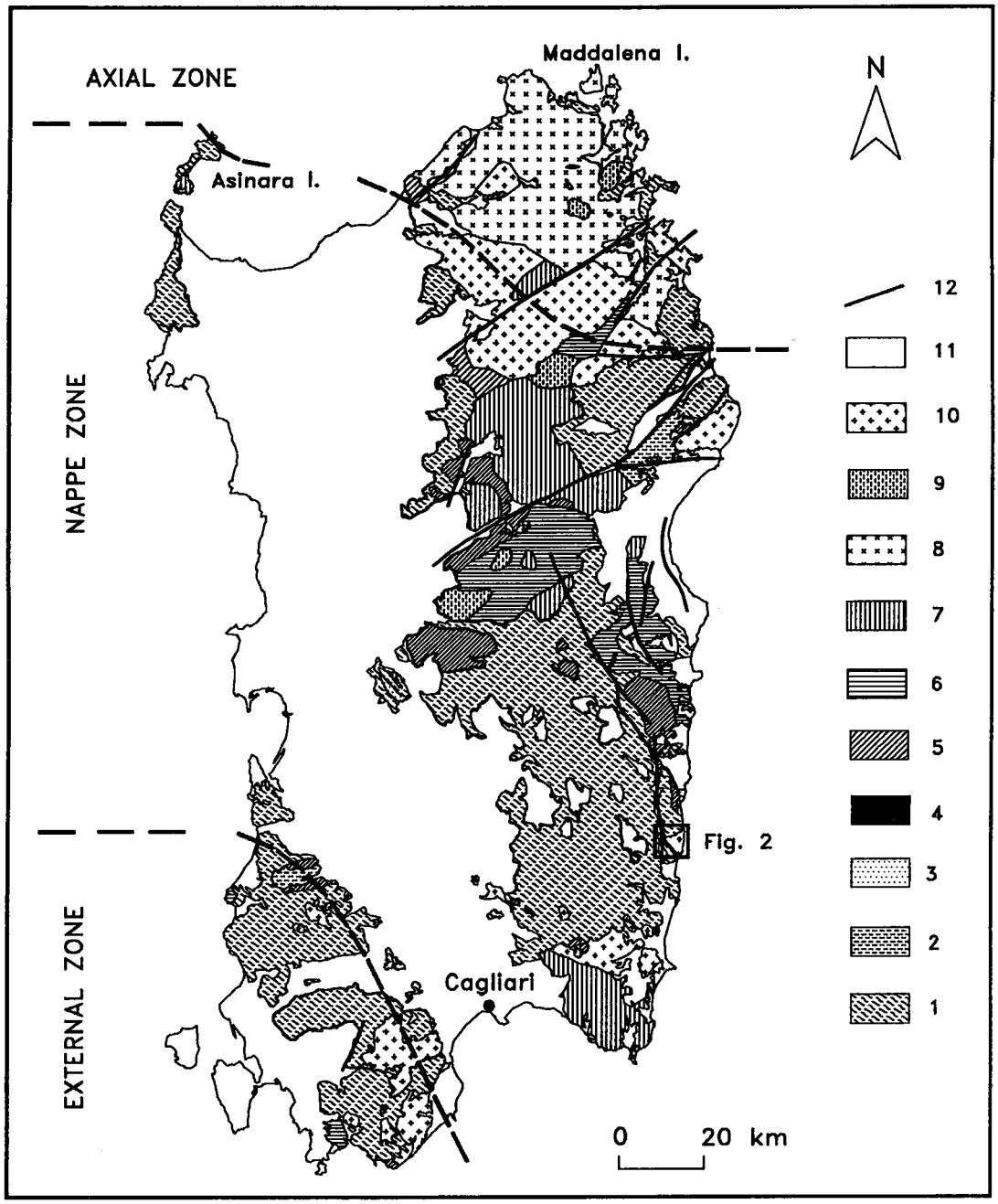

FIG. 1. General geology of Sardinia. Geological base modified after Bralia *et al.* (1982). 1: Metamorphic rocks. 2: Two-mica leucogranite and cordierite-bearing granite. 3: Granite, granodiorite and gneissic tonalite. 4: Tonalitic-gabbroic masses. 5: Tonalite and tonalitic granodiorite. 6: Equigranular monzogranitic biotite-bearing granodiorite. 7: Biotite- and biotite-amphibole-bearing monzogranite and granodiorite. 8: Pink biotite-bearing monzogranite. 9: Equigranular biotite-bearing monzogranite. 10: Pink biotite-bearing leucogranite. 11: Mesozoic, Cenozoic and Quaternary sequences of sedimentary and volcanic rocks. 12: Faults. Box outlines the area of Figure 2.

INTRODUCTION

The occurrence of fayalite in granitic pegmatites is fairly unusual. More commonly, fayalite occurs in silica oversaturated to undersaturated felsic rocks (Frost *et al.* 1988). Fayalite is associated with quartz in highly evolved siliceous volcanic rocks [Mills & Rose (1991), and references therein]; phenocrysts of manganoan fayalite occur for instance in pumice fragments of high-silica rhyolite from the Timber Mountain Tuff, in Nevada. Fayalite also is typical of metamorphosed iron and manganese orebodies.

In Sardinia, Morra *et al.* (1994) recognized fayalite as a primary phase in peralkaline volcanic rocks at Sulcis, southwestern Sardinia, but the only occurrence found so far from a plutonic environment is within pocket pegmatites in leucogranites near Villacidro, southwestern Sardinia (Lovisato 1900). In this paper, we describe manganoan-fayalite-bearing granitic pegmatites in the Quirra region, southeastern Sardinia, in which fayalite occurs as partly altered large crystals, as severely altered crystalline aggregates, and as micrometer-scale largely unaltered drop-like inclusions in quartz. In addition, we describe the relation of the pegmatites to their plutonic host-rocks, post-orogenic Hercynian subsolvus biotite leucogranites of the Mt. Perdosu massif. These granitic rocks characteristically contain fayalite and biotite, and are of a chemical composition that is similar to A-type post-orogenic alkaline granitic suites of the aluminous trend (Bonin 1990). These rocks also have chemical characteristics similar to topaz-bearing rhyolites (Ponce *et al.* 1993). A detailed account of the crystallization history of the fayalite, and its subsequent hydrothermal alteration and weathering, is described elsewhere (Pani *et al.* 1994, Raudsepp *et al.*, in prep.).

GEOLOGICAL SETTING OF SARDINIA

The geology of Sardinia is characterized by various sedimentary and magmatic cycles ranging from early Paleozoic to Recent in age (Fig. 1). The Paleozoic crystalline basement gives its fundamental structure to the Hercynian orogenic cycle (Carmignani *et al.* 1992), which developed by intense deformation, by synkinematic metamorphism, and by an important postcollisional, mainly intrusive magmatic cycle. The Sardinian crystalline basement represents a segment of the south-European Hercynian Chain.

The structural fabric of the crystalline basement is characterized by three belts, referred to as External Zone, Nappe Zone, and Axial Zone, with a NW–SE trend, and a SW to NE zoning with respect to metamorphic grade. These belts represent a tectonometamorphic zoning developed from a low-grade sub-greenschist facies to the greenschist facies (moving from the External to the Nappe zone). The highest grade metamorphic sequence, intruded by late Hercynian magmas, is in the Axial Zone, where the metamorphic grade rapidly increases from greenschist to amphibolite facies with migmatites. Here, the high thermal gradients that were present during the post-collisional event caused widespread anatexis and the emplacement of several bodies of syn-tectonic peraluminous granitic magma.

The Sardinian batholith of Hercynian age (Ghezzo & Orsini 1982) is a typical composite calc-alkaline and subordinately peraluminous batholith that intruded the metamorphic complex produced by the regional Hercynian metamorphism (Fig. 1). Most of this batholith was emplaced at a relatively shallow depth; it is characterized by two cycles of intrusive events. The first cycle yielded syn-and late-tectonic tonalites, granodiorites, monzogranites and leucocratic monzogranite intrusions (Bralia *et al.* 1982); the second cycle is characterized by post-tectonic biotite-bearing leucogranites (Guasparri *et al.* 1984a). According to the classification of Chappell & White (1974), Ghezzo and Orsini (1982) proposed that the Sardinian batholith is characterized mainly by "I"-type, and, subordinately, "S"-type plutonic rocks. Also, these features distinguish the Sardinian batholith from the other European Hercynian batholiths, which seem to be predominantly of "S"-type (Pitcher 1979), although the abundance of the I-type granitic bodies is quite considerable (Finger & Steyrer 1990). However, in our study area, the Mt. Perdosu granitic massif exhibits chemical characteristics more like those of A-type post-orogenic alkaline granitic suites of the aluminous trend (Bonin 1990).

EXPERIMENTAL METHODS

Electron-probe micro-analyses of fayalite (Table 1) were done on a fully automated CAMECA SX–50 microprobe, operating in the wavelength-dispersion mode, with the following operating conditions: excitation voltage 15 kV, beam current 20 nA, peak count

TABLE 1. SELECTED RESULTS OF ELECTRON-PROBE MICROANALYSES OF MANGANOAN FAYALITE, QUIRRA, SARDINIA

	1	2	3	4	5
SiO_2 wt.%	29.83	29.04	29.58	29.59	30.57
FeO	63.17	64.49	61.80	52.14	57.23
MgO	1.15	1.23	0.63	0.24	0.23
MnO	5.76	5.37	7.79	18.50	11.47
Total	99.91	100.13	99.80	100.47	99.50
	Number of ions on the basis of 4 O				
Si	1.00	0.98	1.00	1.00	1.03
Fe^{2+}	1.78	1.82	1.75	1.47	1.61
Mg	0.06	0.06	0.03	0.01	0.01
Mn	0.16	0.15	0.22	0.53	0.33
Total	3.00	3.02	3.00	3.00	2.97

1. Fayalite from unaltered core of large zoned crystal.
2. Fayalite from unaltered part of smaller unzoned crystal.
3. Drop-like fayalite from composite aggregate.
4. Drop-like fayalite from composite aggregate.
5. Drop-like fayalite from associated leucogranite.

TABLE 2. MAJOR-ELEMENT CHEMICAL COMPOSITION OF SELECTED QUIRRA FAYALITE-BEARING GRANITIC ROCKS

	Q11	L7	Q23/3	Q10	Q18	Q29
SiO_2 wt.%	75.69	75.83	75.36	76.73	77.30	76.31
TiO_2	0.11	0.06	0.04	0.05	0.02	0.03
Al_2O_3	13.11	12.68	13.77	12.70	12.87	13.32
Fe_2O_3*	1.46	1.69	1.10	1.40	0.97	1.06
MnO	0.07	0.12	0.04	0.04	0.04	0.06
MgO	0.16	0.03	0.01	0.01	< d.l.	< d.l.
CaO	0.77	0.65	0.26	0.34	0.21	0.23
Na_2O	3.56	3.05	3.60	3.20	4.18	3.68
K_2O	4.58	4.92	5.01	4.86	4.04	5.00
P_2O_5	0.03	0.02	0.01	0.02	0.02	0.01
L.O.I.	0.56	0.92	0.66	0.71	0.55	0.48
Total	100.10	100.05	99.89	100.08	100.20	100.19
	C.I.P.W. normative minerals					
Qtz	35.54	37.73	35.19	38.75	37.05	35.23
Crn	0.92	1.13	2.41	1.57	1.26	1.44
Or	27.19	29.24	29.71	28.82	24.00	29.68
Ab	30.12	25.81	30.46	27.07	35.37	31.14
An	3.73	3.26	0.00	1.62	0.94	1.08
A.S.I.	1.07	1.10	1.21	1.14	1.11	1.12

A.S.I. = alumina saturation index $(Al_2O_3)/(CaO+Na_2O+K_2O)$; *total iron as Fe_2O_3.

time 20 s, background count time 10 s, beam diameter 1 μm. Data reduction was done with the "PAP" $\phi(\rho Z)$ method (Pouchou & Pichoir 1985). For the elements sought, the following standards, X-ray lines and crystals were used: synthetic Mg_2SiO_4, Mg*K*α, TAP; synthetic Fe_2SiO_4, Si*K*α, TAP, Fe*K*α, LIF; synthetic $MnSiO_3$, Mn*K*α, LIF. The following elements were sought but not detected: Na, Al, Ca, Cr, Ni.

Whole-rock major-element analyses (Table 2) were done by X-ray fluorescence spectrometry using the fusion method. FeO was determined using ammonium metavanadate titration. Trace-element analyses (Table 3) were done by fusion-mode inductively coupled plasma – mass spectrometry; the concentration of Li was established using total digestion.

Textural and Compositional Details Concerning the Fayalite and its Alteration Products

The manganoan-fayalite-bearing granitic pegmatites considered here are similar in mineralogical aspects to those previously described in the literature. Janeczek (1989) outlined in detail the multi-stage hydrothermal alteration of anhedral fayalite (up to 9 cm in diameter) from unzoned schlieren pegmatites up to 0.5 m wide in biotite–hornblende Hercynian granite near Strzegom, Lower Silesia. The fayalite there is surrounded by microcline, has a manganoan greenalite – magnetite rim, and a manganoan grunerite – magnetite – manganoan minnesotaite outer zone in a stilpnomelane- or greenalite-rich groundmass. In the fayalite-bearing pegmatites from the Sawtooth batholith, central Idaho, fayalite occurs as euhedral crystals intergrown with quartz, orthoclase, and albite (Hirt 1991). Buda (1993) described fayalite from coarse-grained pegmatitic "nests" 15–25 cm in diameter occurring with basic enclaves in a monzogranitic intrusion of Hercynian age; here the fayalite is found as anhedral to euhedral prismatic crystals measuring 4 × 6 mm. Palache (1950) summarized the occurrence of fayalite at four localities at Cape Ann, Massachusetts. Although all of the fayalite is found in various granitic pegmatites, the evidence presented suggests that the pegmatites are not related to the Rockport granite, but are xenoliths probably related to an earlier fayalite-bearing quartz-bearing syenite.

In southeastern Sardinina, bodies of fayalite-bearing granitic pegmatite occur at the northwestern margin of the Mt. Perdosu massif (Fig. 2); the largest and most differentiated are best exposed in an erosional window (Figs. 2, 3) cutting through the overlying Ordovician–Silurian metasedimentary rocks into which the Mt. Perdosu massif had been intruded. Smaller bodies of pegmatite also occur scattered near the northern contact between the metasedimentary rocks and the main exposure of the massif (Figs. 2, 3). The absolute age of the pegmatites has not been determined, but field, mineralogical and geochemical data suggest that they are post-orogenic and closely related to the Hercynian leucogranites.

The pegmatites occur as lenses, veinlets and pocket-shaped bodies. All are hosted by the granite close to the contact with the metasedimentary rocks, which suggests that the pegmatites crystallized in the upper part of the cupola of the host pluton (Fig. 3). Two types of pegmatite bodies are exposed: (i) a large lens-shaped body with partly altered crystals of manganoan fayalite ("main" pegmatite, Fig. 3, Unit 8); (ii) numerous small, variously shaped bodies with or without fayalite, and a subhorizontal pegmatitic facies, a grain-size variation of the granitic pluton ("other" pegmatites, Fig. 3, Units 5, 6, 7). Selected results of electron-probe microanalyses of manganoan fayalite from the pegmatites and host granitic rocks are given in Table 1.

Main pegmatite

The lens-shaped main pegmatite (Fig. 3, Unit 8) is found in the fine-grained leucogranite (Fig. 3, Unit 3), trends northwest–southeast, measures 20 × 60 m, and contains abundant large crystals and crystalline aggegates of manganoan fayalite. The contact with the wallrock is generally straight and sharp, but is locally complexly contorted and diffuse. Also present in the main pegmatite is microcline, albite, quartz, and biotite. Muscovite occurs as aggregates of fine crystals or fills fractures, mainly in quartz and alkali feldspar.

Abundant occurrences of manganoan fayalite are found along the upper part of the pegmatite in three typical habits: (i) spectacular large anhedral to subhedral single crystals or composite groups of a few

individuals up to 15 × 30 cm in size enclosed by microcline and variously altered by subsolidus, hydrothermal and weathering processes (Figs. 4A, B); (ii) smaller, more or less completely altered irregular aggregates of several crystals up to a few cm in size enclosed by microcline (Fig. 4C); (iii) micrometer-scale drop-like inclusions in quartz in composite aggregates consisting of biotite, chlorite, quartz, and rare muscovite (Fig. 4D). Notably, such drop-like crystals of fayalite also occur in the quartz of the host leucogranite adjacent to the pegmatite bodies.

Although some of the large crystals of fayalite seem to be aggregates, the best example of this type is optically continuous in all of its unaltered parts and appears to have been a single subhedral crystal imbedded in microcline (Fig. 4A). The degree of alteration of the larger crystals (15 × 30 cm range) is controlled by the size of the crystal, its cleavage and by fractures. The

TABLE 3. TRACE-ELEMENT CHEMICAL COMPOSITION OF SELECTED QUIRRA FAYALITE-BEARING GRANITIC ROCKS

	Q11	L7	Q23/3	Q10	Q18	Q29
Ni ppm	5.0	12.0	13.0	21.0	8.0	21.0
Pb	44.0	66.0	32.0	40.0	65.0	80.0
Zn	57.0	131.0	94.0	114.0	39.0	146.0
Bi	< d.l.	0.4	< d.l.	0.1	4.7	0.5
Sn	7.0	15.9	7.4	3.8	9.2	21.9
W	1.4	2.7	0.9	1.5	2.8	2.2
Mo	2.3	3.3	2.4	4.0	2.2	2.5
Rb	277.2	410.9	245.4	240.0	309.6	341.5
Cs	4.3	4.3	2.8	3.4	2.8	3.6
Ba	264.2	467.9	96.6	105.4	30.9	53.8
Sr	38.8	25.5	31.5	16.9	9.4	11.1
Tl	1.7	3.4	2.1	2.0	1.8	3.0
Ga	19.0	22.0	21.0	20.0	24.0	23.0
Li	151.0	120.0	36.0	37.0	28.0	32.0
Be	7.0	2.0	3.0	2.0	10.0	3.0
Ta	2.9	2.4	1.0	2.4	6.5	4.8
Nb	12.9	14.3	7.9	15.1	23.2	19.2
Hf	3.8	4.0	2.1	3.4	3.6	4.5
Zr	88.6	80.1	37.1	63.9	47.2	68.4
Th	23.2	29.4	18.0	29.6	21.8	25.5
U	6.5	5.6	4.0	12.7	7.4	11.1
Y	65.5	83.2	24.8	64.6	103.8	81.9
La	23.5	17.4	12.0	13.2	15.1	13.9
Ce	53.0	41.8	26.1	31.0	35.8	34.0
Pr	6.3	4.4	2.7	3.2	5.3	3.6
Nd	26.6	25.4	15.3	18.3	25.1	20.1
Sm	8.8	8.4	4.3	5.9	11.8	7.3
Eu	0.40	0.18	0.32	0.20	0.03	0.10
Gd	8.8	9.2	4.5	7.2	14.5	9.3
Tb	2.0	1.9	0.8	1.5	3.4	1.9
Dy	10.2	12.8	4.5	10.2	17.8	13.4
Ho	2.2	2.6	0.9	2.1	3.8	2.8
Er	7.1	8.5	2.8	6.6	12.3	8.7
Tm	1.2	1.4	0.4	1.1	2.0	1.4
Yb	7.4	9.3	2.7	6.8	13.6	9.8
Lu	1.1	1.5	0.4	1.1	1.9	1.6
ΣREE	158.6	144.8	77.7	108.4	162.4	127.9
ΣLREE	118.6	97.5	60.7	71.8	93.1	79.0
ΣHREE	40.0	47.2	17.0	36.6	69.3	48.9
$(La/Sm)_n$	1.7	1.3	1.8	1.4	0.8	1.2
$(Gd/Lu)_n$	1.0	0.7	1.3	0.8	1.0	0.7
$(La/Lu)_n$	2.2	1.2	3.0	1.2	0.8	0.9
Nb/Ta	4.2	6.0	7.9	6.3	3.6	4.0
Ga/Al	2.7	3.3	2.9	3.0	3.5	3.3

n.d. = not determined; d.l. = detection limit.

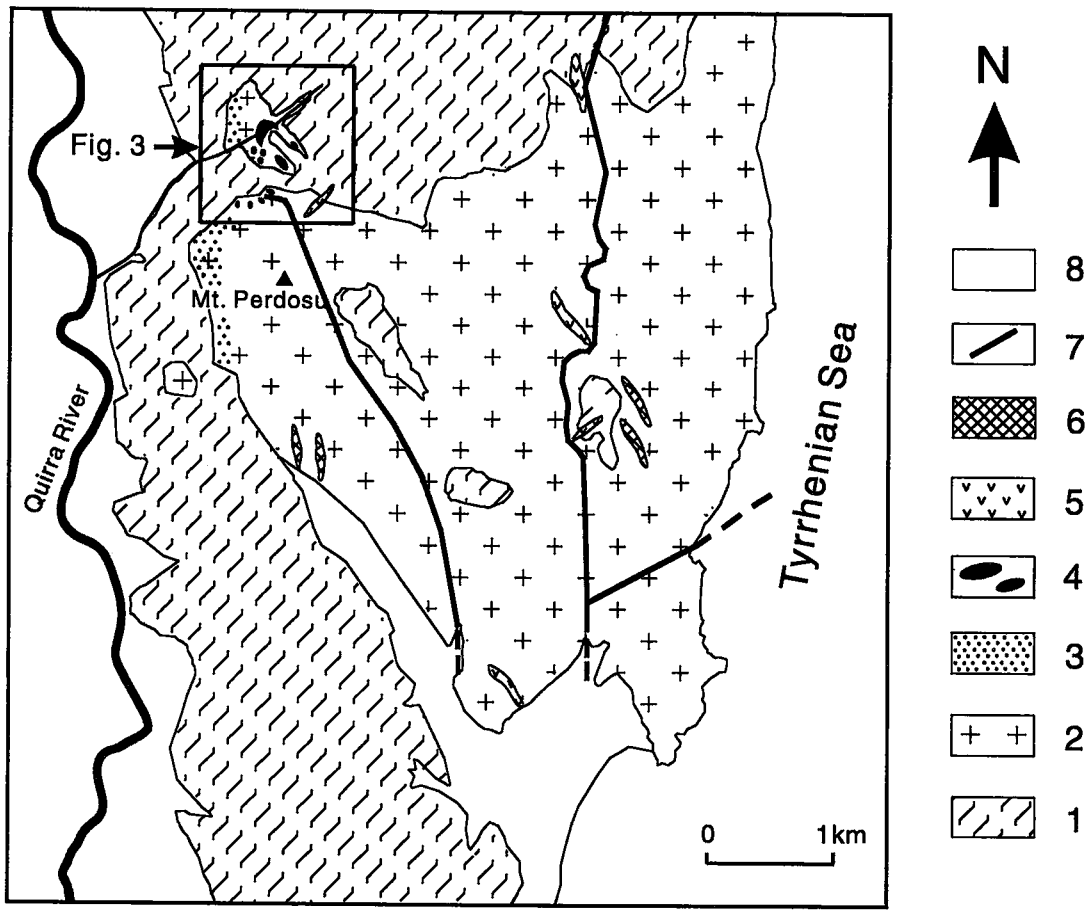

FIG. 2. Geological sketch map of Mt. Perdosu granitic massif and the fayalite-bearing pegmatites. 1. Ordovician–Silurian metasedimentary rocks. 2. Granitic rocks. 3. Greisen. 4. Pegmatites. 5. Basic subvolcanic dikes. 6. Hydrothermal lodes. 7. Faults. 8. Recent alluvial deposits. Box outlines the area of Figure 3.

largest crystal exhibits three primary zones: core, intermediate zone, and rim (Fig. 4B). The core is clear, colorless to pale yellow fayalite, invariably optically continuous, and with sparsely scattered enclosed aggregates of grunerite + magnetite ± greenalite that are least abundant at the core. Along well-developed cleavages and near fractures, the fayalite is of a darker yellow to pale reddish brown color due to oxidation. Locally, there are veins filled with greenalite, calcite and Fe-rich sphalerite. The Mn content of the unaltered core, having the structural formula $(Fe_{1.78}Mg_{0.06}Mn_{0.16})Si_{1.00}O_4$, varies between 5 and 6 wt.% MnO (Table 1, No. 1).

The rim consists mainly of various phyllosilicate minerals, of which anhedral green to pale brown-green to dark brown-green pleochroic biotite [Fe/(Fe + Mg) = 0.85] is the most abundant. At the outermost edge, the biotite is deformed and mixed with very fine-grained, Fe-rich red-brown to opaque mica-like material. At the boundary with, and in some cases extending into the intermediate zone, ferripyrophyllite occurs as anhedral dark yellow, nonpleochroic grains. Subhedral magnetite and anhedral quartz grains also occur scattered throughout the rim.

The intermediate zone comprises the major part of the crystal, and is generally concentric about the core (Fig. 4B). However, because of a major fracture, the intermediate zone cuts the core into two parts (Fig. 4B). The intermediate zone consists essentially of micrometer-scale intergrowths of laihunite, iron oxides and hydroxides. In some previous studies (*e.g.*, Janeczek 1989), this material has been described as "iddingsite". We have positively identified the bulk of

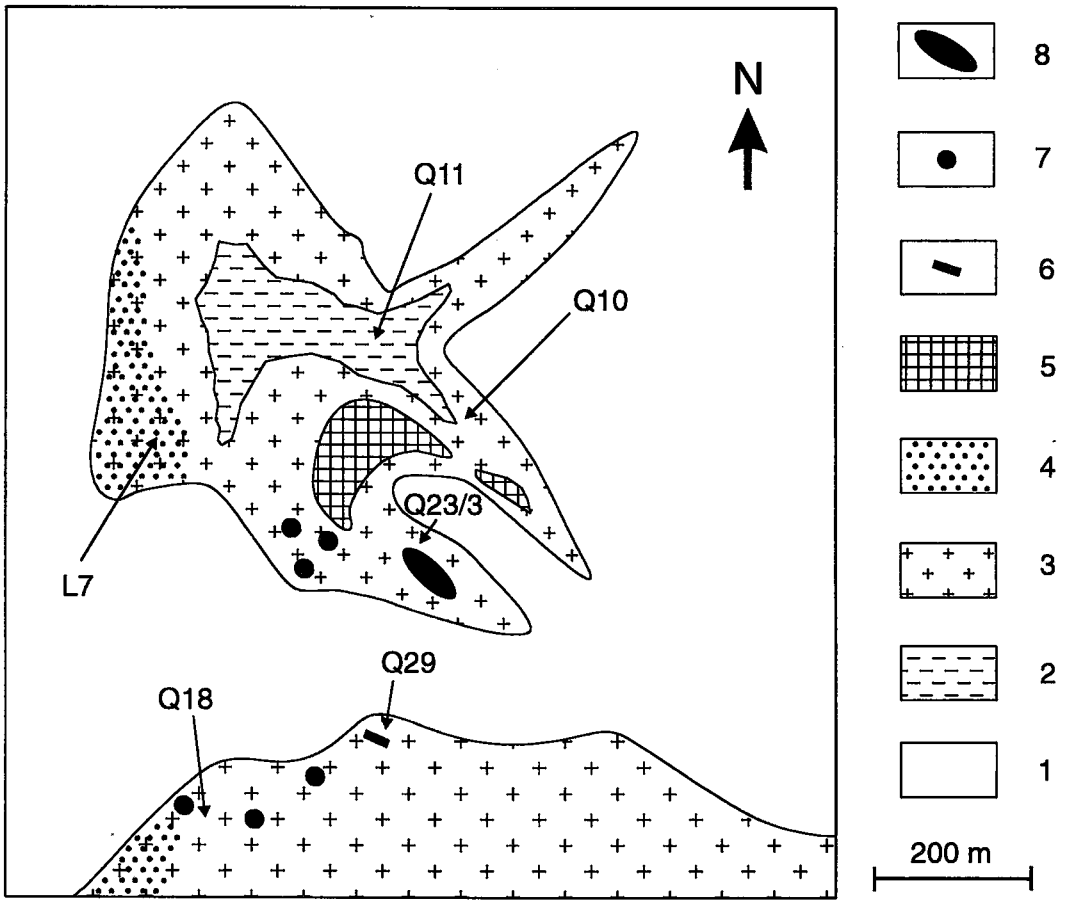

FIG. 3. Detailed geology of the pegmatite locality, showing sample locations. Host rocks: 1. Ordovician–Silurian metasedimentary rocks. 2. Medium-grained leucogranite. 3. Fine-grained leucogranite. 4. Greisen, pegmatites. 5. "Other" euhedral quartz, alkali feldspar pegmatite facies. 6. "Other" 6 × 11 m lens-shaped pegmatite. 7. "Other" altered fayalite-bearing pegmatites. 8. "Main" fayalite-bearing pegmatite.

the alteration product to be laihunite from X-ray diffraction and electron-probe micro-analysis. The presence of significant Fe^{3+} in fayalite from a variety of rocks (including granitic pegmatite) due to finely intergrown laihunite has been documented by others (*e.g.*, Schaefer 1983, 1985).

Near the rim, the intermediate zone contains abundant magnetite with small grains of quartz, and large, irregular patches of brown-stained but generally colorless grunerite. Further away from the rim, grunerite is present only as isolated acicular and prismatic grains, generally with magnetite, minor quartz and rare greenalite. The contact with the core is very irregular, but shows clearly that the alteration of the fayalite was controlled by the fractures and its cleavage. The Mn content of unaltered parts of the intermediate zone is similar to that of the core, varying between 5 and 6 wt.% MnO.

Irregular aggregates of fayalite occur also only in microcline, and are probably smaller equivalents of the large crystals described above (Fig. 4C). Their morphology and mineralogy are different by virtue of severe to complete alteration of a smaller volume of primary material. These grey to dark green to brown aggregates are also characterized by a rim of biotite, mixed with chlorite and magnetite. Because of the small size of the aggegates, the alteration assemblages are not zoned as in the large crystals, but consist of complex mixtures of some relatively unaltered fayalite (rare), laihunite, iron oxides and hydroxides not yet defined,

magnetite, grunerite, greenalite, plus phases not related to fayalite, such as kaolinite and unidentified clays. Typical bulk Mn contents vary between 3 and 9 wt.% MnO.

Micrometer-scale drop-like inclusions of fayalite in quartz are found in composite aggregates consisting essentially of biotite, chlorite, quartz, and rare muscovite (Fig. 4D). The MnO content of individual inclusions of fayalite, in round to amoeboid grains, varies between 7 and 19%, *i.e.*, much more and more variable than the fayalite described above (Table 1). Most of these drop-like inclusions of fayalite are monomineralic; some, however, have magnetite and greenalite at the fayalite–quartz boundary (Fig. 5A). These drop-like inclusions provide the clearest evidence of magmatic crystallization of the fayalite. Drop-like crystals of fayalite in quartz in the associated granitic rocks also have high Mn content, about 12 wt.% MnO (Table 1, No. 5). The Mg content of drop-like fayalite in both the aggregates and granitic rocks is significantly lower (about 0.2–0.6 wt.% MgO) than those of the larger crystals (about 1.2 wt.% MgO).

Other pegmatites

Numerous small veins, pockets and lens-shaped bodies (1–11 m in length) of pegmatite are found within about 600 m of the main pegmatite. Some occur adjacent to the main pegmatite and are exposed by the erosional window in the metamorphic rocks; others are at the contact between the massif and the metamorphic rocks to the south (Figs. 2, 3).

Near the greisen facies at the northwest margin of the main pegmatite (Fig. 3), there is a subhorizontal pegmatitic facies, which is developed as a grain-size variation of the granitic pluton; it comprises massive quartz

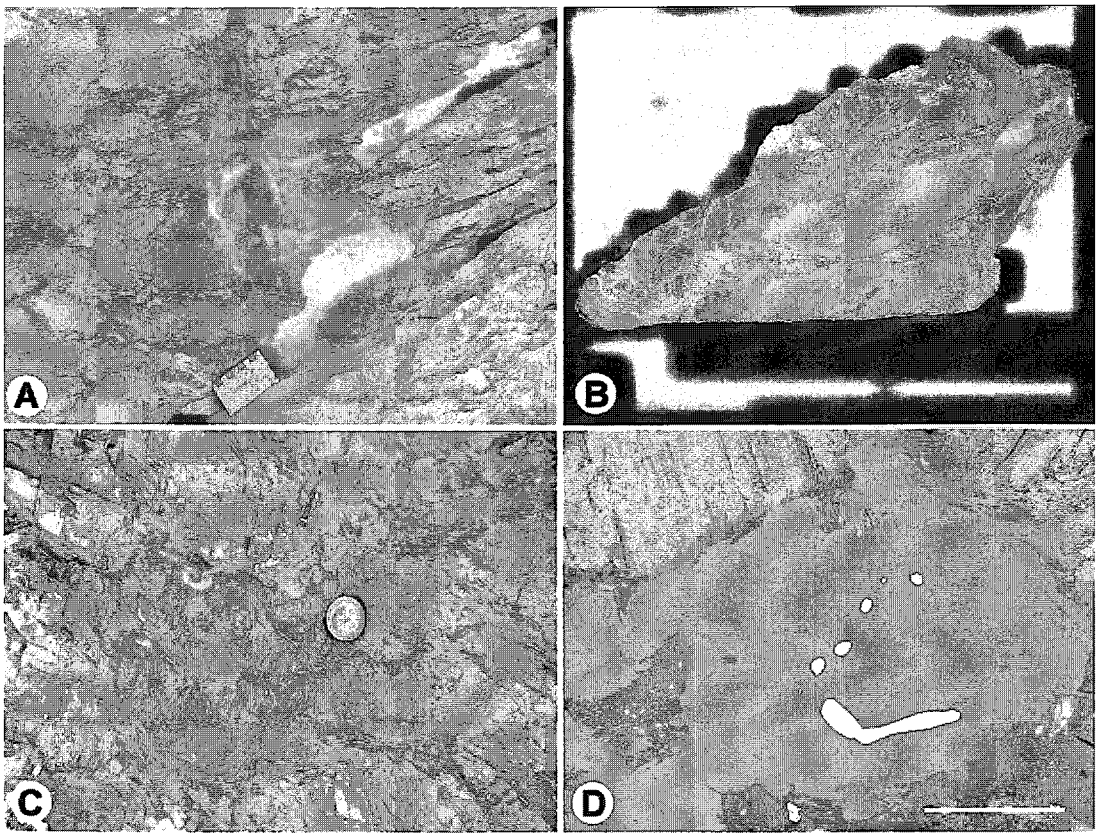

FIG. 4. A. Typical large crystals of fayalite in potassium feldspar. Scale card marked in cm. B. Photograph of cut surface through the center of a typical large crystal of fayalite (30 cm long) showing the unaltered core (pale grey), partly to completely altered intermediate zone (dark grey to black), and micaceous rim (mostly missing). Note the fracture-control of the degree of alteration, and veins of calcite, greenalite and sphalerite (pale grey to white). C. Altered irregular aggregate of fayalite with a rim of dark mica. Coin is about 2 cm in diameter. D. Back-scattered electron image of drop-like fayalite inclusions (white) in quartz (grey) from composite quartz – biotite – chlorite aggregate. Scale bar: 100 μm.

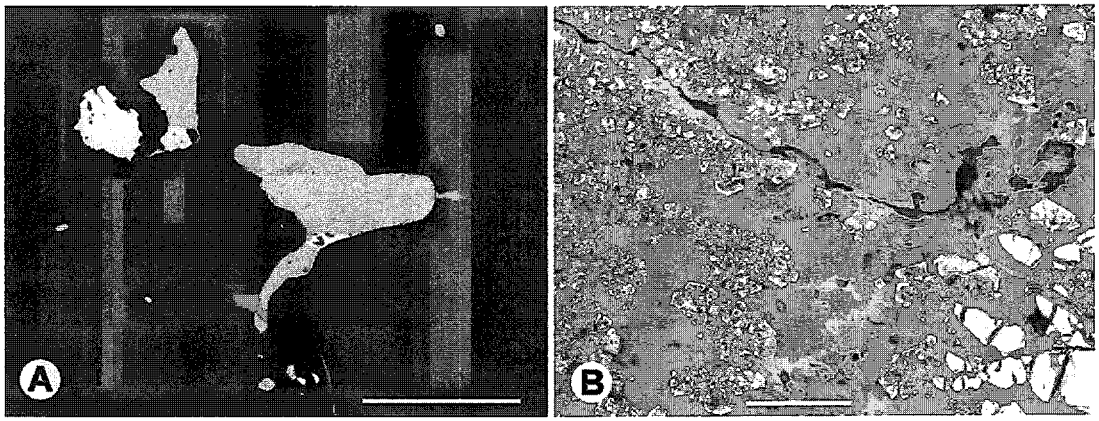

FIG. 5. A. Back-scattered electron image of drop-like fayalite (light grey) with magnetite (white) and greenalite (medium grey) included in quartz (dark grey). Scale bar: 100 μm. B. Back-scattered electron image of magnetite (white) + quartz (medium grey) and secondary iron oxides and hydroxides (light grey) in aggregate from 6 × 11 m "other" pegmatite. Scale bar: 200 μm.

and large euhedral crystals (>10 cm), microcline, and irregular aggregates (up to 10 cm) of alteration products after fayalite. These aggregates are complex intergrowths of magnetite + grunerite + quartz scattered throughout a groundmass that has a composition identical to that of fayalite. In the pegmatite, the quartz is present both as euhedral crystals (>10 cm) perpendicular to the projected contact with the overlying metasedimentary rocks and as anhedral masses.

The largest of the "other" pegmatites is a 6 × 11 m lens-shaped body at the contact between metamorphic rocks and fine-grained leucogranite (Fig. 3). The major minerals are massive microcline and euhedral quartz up to 10 cm in diameter. Scattered throughout the microcline are aggregates of intergrown magnetite + quartz (4–5 cm in size). The magnetite occurs with two habits: skeletal intergrowths with porous quartz, and anhedral to subhedral crystals embedded in larger, massive quartz (Fig. 5B). The quartz–magnetite intergrowths contain abundant secondary iron oxides in fractures and filling cavities. The magnetite–quartz aggregates in this pegmatite contain no material that appears to be altered fayalite.

The other small veins, pockets and lens-shaped bodies of pegmatite up to 3 m long are similar in mineralogy. Quartz and feldspar are the main constituents, with scattered magnetite + quartz and magnetite + quartz + grunerite aggregates up to 5 cm long and similar to those described above. Locally, unidentified mica-like minerals (probably clays and ferripyrophyllite) and mixtures of iron oxides and hydroxides are abundant products of weathering. Some of the aggregates are rich in fayalite, now altered to a mixture of laihunite and various oxides and hydroxides. Notably, some of the magnetite + grunerite intergrowths also contain fine-grained grunerite + magnetite symplectite.

GEOLOGY AND GEOCHEMISTRY OF THE ASSOCIATED GRANITIC ROCKS

In general, the Quirra granites belong to the Mo–W specialized Sardinian leucogranite suite (Ghezzo *et al.* 1981, Guasparri *et al.* 1984b). The Mt. Perdosu massif comprises plutons of post-orogenic monzogranites and leucogranites, which were emplaced at a shallow level in the crust in a distensive regime at the end of the Hercynian orogeny (Biste 1979, Bralia *et al.* 1982, Guasparri *et al.* 1984a). All of these granitic rocks and related pegmatites intruded the Ordovician–Silurian metasedimentary rocks belonging to the Gerrei tectonic units (Carmignani *et al.* 1986); they are now generally metamorphosed to hornfelses and skarn-type facies.

The portion of the Mt. Perdosu massif exposed in the erosional window has a well-defined vertical zoning in texture and mineralogy (Fig. 3). The most internal leucogranite is typically medium- to coarse-grained subsolvus biotite leucogranite (Fig. 3, Unit 2), which grades into a fine-grained facies toward the external part of the pluton (Fig. 3, Unit 3), together with a greisen-type facies (Fig. 3, Unit 4) where muscovite predominates over biotite (Biste 1979). Upward, the same fine-grained leucogranite grades into a subhorizontal pegmatitic facies characterized by euhedral quartz crystals (>10 cm) perpendicular to the contact, together with massive microcline (Fig. 3, Unit 5). The last stage of consolidation of the granitic magma is represented by the emplacement of the pegmatite bodies (Fig. 3, Units 6, 7, 8).

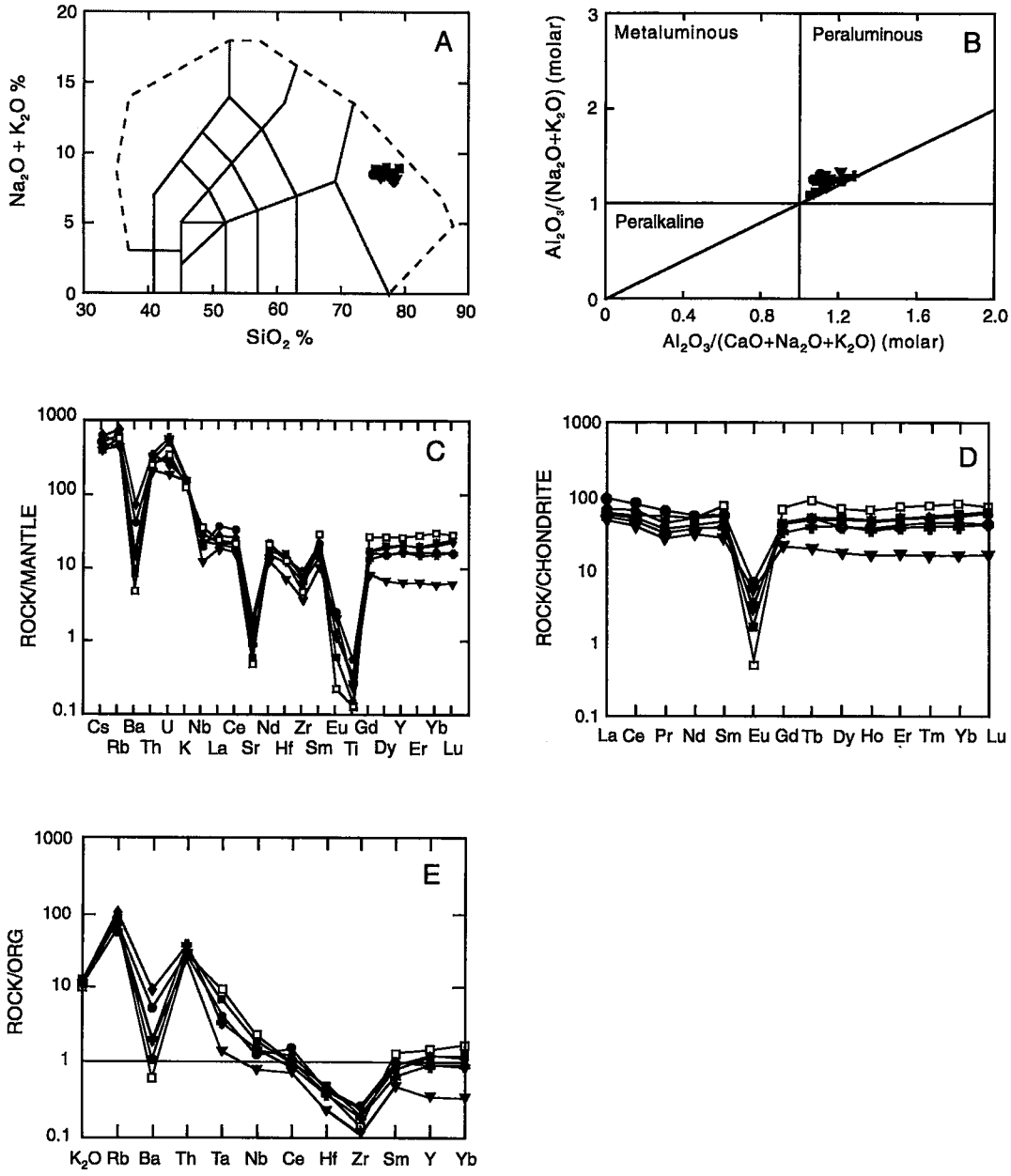

FIG. 6. Chemical characteristics of Quirra granites using A. Total alkali *versus* silica plot (TAS) (Middlemost 1994) (● medium-grained leucogranite, ■ fine-grained leucogranite, ◆ medium grained leucogranite associated with greisen, ▼ fine-grained leucogranite associated with main pegmatite, + fine-grained leucogranite associated with euhedral quartz, alkali feldspar pegmatite facies). B. alumina saturation diagram (Maniar & Piccoli 1989). Symbols as for Figure 6A. C. Primitive-mantle-normalization diagram (Sun 1982) (● Q11, + Q10, ■ Q29, □ Q18, ◆ L7, ▼ Q23/3). D. Chondrite-normalized *REE* patterns [normalization values after Evensen *et al.* (1978)]. Symbols as for Figure 6C. E. Ocean-ridge-granite-normalized element patterns (Pearce *et al.* 1984). Symbols as for Figure 6C.

The mineralogy (compositions determined by electron-probe micro-analyses) of the granites associated with the pegmatites consists mainly of quartz, microcline (Or_{91-99}) with or without an obvious perthitic texture, plagioclase (An_{19-1}), biotite [Fe/(Fe + Mg) in the range 0.81–0.95; $Al_{tot.}$ in the range 3.2–5.3 (22 O)] and minor muscovite. Accessory minerals include fayalite, zircon, apatite, fluorite, rarely sphalerite and other sulfides, niobian rutile, xenotime-(Y) and monazite-(Ce). In the total alkali *versus* silica diagram (Fig. 6A), the Quirra suite plots within the monzogranite field. Di Simplicio *et al.* (1974), Bralia *et al.* (1982), and Guasparri *et al.* (1984a) considered these rocks to be leucogranitic owing to their low content of mafic minerals (modal content of biotite < 5 vol.%).

Results of major- and trace-element whole-rock analyses, and normative mineralogy of representative samples of each granitic facies, are given in Tables 2 and 3. These rocks are characterized by high SiO_2 contents (>75 wt.%), low Ca (<0.81 wt.% CaO), Al (<13.77 wt.% Al_2O_3) and high FeO_{tot}/MgO (8–140) and high alkali abundances ($Na_2O + K_2O$ in the range 7.72–8.68 wt.%). Moreover, they are peraluminous, as shown by their position on the alumina saturation diagram of Maniar & Piccoli (1989) (Fig. 6B), together with normative corundum contents (0.71–2.52 wt.%, Table 2).

Trace-element concentrations in these granites are characteristic of a generally high degree of fractionation. Selected samples representative of the granitic facies are plotted on spider diagrams (Fig. 6). Ba and Sr contents are very low (Fig. 6C, Table 3), except for the medium-grained leucogranite facies (Q11, Fig. 3, Unit 2) and for the associated greisen facies (L7, Fig. 3, Unit 4). This is to be expected, as they are probably derived from an earlier, less differentiated facies. Furthermore, Cs (<12 ppm), Rb (<456 ppm), and U (<14 ppm) (Fig. 6C, Table 3), and Be (<10 ppm) and Li (<181 ppm) (Table 3) are relatively high.

In spite of both the highly fractionated and peraluminous character of the magmas from which these leucogranites crystallized, concentrations of the rare-earth elements (*REE*) are low (total *REE* in the range 33–190 ppm). All the samples are slightly enriched in the light rare-earth elements (*LREE*) comparison to the heavy rare-earth elements (*HREE*) (Table 3). In a plot of chondrite-normalized abundances (Fig. 6D), the *REE* fractionation among the selected samples of the granitic facies is evident; the more depleted trend is shown by the granite sample intimately associated with the main pegmatite; also, the *LREE* and *HREE* fractionation is not pronounced, as well indicated by $(La/Sm)_n$, $(Gd/Lu)_n$ and $(La/Lu)_n$ values (0.8–1.7, 0.7–1.3, and 0.8–3.0, respectively: Table 3). The flat *REE* patterns indicate that there was little or no fractionation of *REE*-bearing minerals, and that *LREE*- and *HREE*-selective phases are both present (Rizzo *et al.* 1996). Furthermore, all samples show a pronounced negative Eu anomaly, likely due to fractionation of mainly feldspar or Eu-bearing accessory minerals [*e.g.*, monazite-(Ce)].

In the tectonic discrimination plot (Fig. 6E) on which compositions are normalized to ORG (Pearce *et al.* 1984), the Quirra leucogranites show a geochemical affinity with granites belonging to collisional geodynamic environments. However, there is a significative shift of some elements from the general pattern. In particular, Ba (especially for samples Q18 and Q29) is relatively depleted, Sm, Y and Yb are enriched, and Ta and Nb show slight enrichment. These shifts can be explained by the fact that crystal fractionation was probably an important mechanism in the genesis of these granites, during which Ba depletion was caused by the fractionation of feldspar, and the Sm, Y and Yb enrichment was a result of incorporation into minerals rich in these elements [*e.g.*, xenotime-(Y)]. Ta and Nb enrichments can be explained by the lack of fractionation of a phase that hosts these elements (*e.g.*, niobian rutile).

Most of the samples display geochemical features of "within-plate" granites (Figs. 7A, B), and in general all of them plot in the field of the "post-collisional" granites. The observed depletion of high field-strength elements (*HFSE*) in samples from the granitic facies intimately associated with the main and subhorizontal pegmatites (Fig. 3), shifts their positions to the VAG + syn-COLG field. This shift could be attributed to a "dilution" of these elements by a "pegmatite effect" from a possible loss of a volatile phase, as also proposed by Pearce *et al.* (1984). Evidence of this effect is found in the presence of fluorite crystals enclosed by plagioclase and quartz in most of the granite samples, and by the occurrence of fluorite with sulfides (*e.g.*, sphalerite, pyrite, chalcopyrite, galena) in the main pegmatite samples. The "within plate" features are typical of A-type granites (Loiselle & Wones 1979, Collins *et al.* 1982, Whalen *et al.* 1987, Eby 1990, 1992). To test whether our granitic rocks belong to the A-type suite, compositions were plotted on discrimination diagrams (Figs. 7C, D, E; Fig. 8) that make use of certain combinations of major and trace elements (*e.g.*, Whalen *et al.* 1987, Eby 1990). According to Eby (1990), the effective discriminant between A-type and I- and S-type granitic rocks is the FeO_{tot}/MgO *versus* SiO_2 diagram. In our samples, the FeO_{tot}/MgO value is in the range 8–140, and they plot in the A-type field on Figure 7C. Eby (1992) distinguished two sub-groups of A-type granites on the basis of Y/Nb ratio. The Y/Nb ratio in these samples is in the range 1.4–6.7, and they plot in the A_2-type field (Figs. 7D, E). Furthermore, according to the F1 *versus* F2 major-element discriminant functions of Ponce *et al.* (1993), these leucogranites are derived from parent magmas that can be related to those of topaz-bearing rhyolites (Fig. 7F).

An examination of the behavior of Ga/Al, Zr, Nb, Ce, Y and various major-element ratios (Figs. 8A–L)

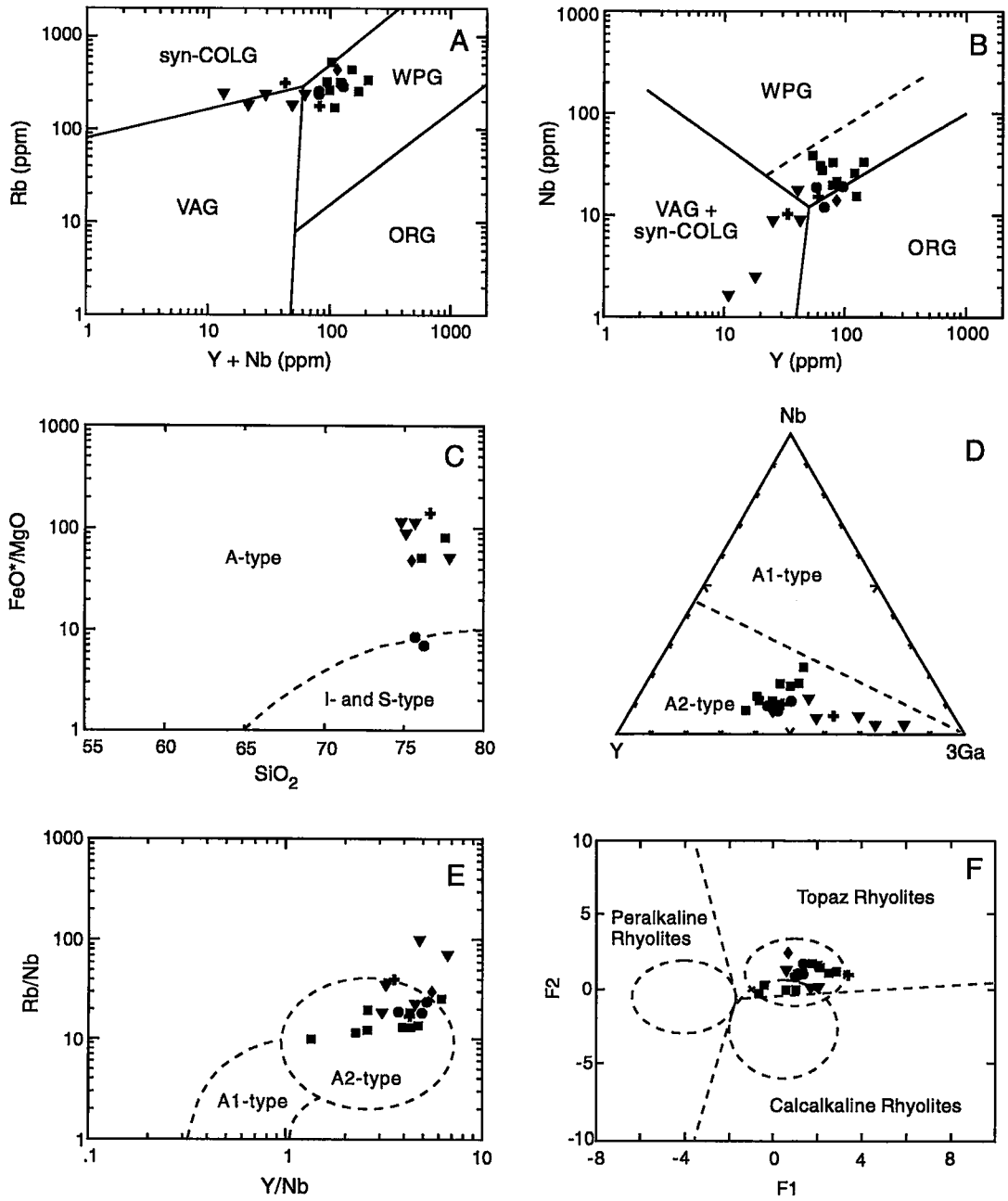

FIG. 7. A, B. Rb *versus* Y + Nb and Nb *versus* Y tectonic discrimination diagrams (Pearce *et al.* 1984) (VAG, volcanic arc granites; syn-COLG, syn-collisional granites; WPG, within-plate granites; ORG, ocean-ridge granites). C. FeO*/MgO *versus* SiO_2 diagram (Eby 1990). The dashed line represents the field of the I- and S-type granites. D. Y–Nb–Ga*3 diagram (Eby 1992) (A1-type, anorogenic rifting-phase tectonic settings; A2-type, postorogenic tectonic settings). E. Rb/Nb *versus* Y/Nb diagram (Eby 1992) (A1-type, anorogenic rifting-phase tectonic settings; A2-type, postorogenic tectonic settings). F. F1 *versus* F2 major-element discriminant functions (Ponce *et al.* 1993), showing fields for calc-alkaline, peralkaline and topaz rhyolites. Ellipses enclose areas in which 95% of the type samples plot. Symbols: as for Figure 6A.

shows that the chemical compositions of these granites are consistent with the compositions of the subsolvus postorogenic A-type granites of the aluminous trend, although the Quirra granites are characterized by a lower content of some trace elements (especially Zr and Ce) than the A-type granites of the peralkaline trend (Bonin 1988, 1990).

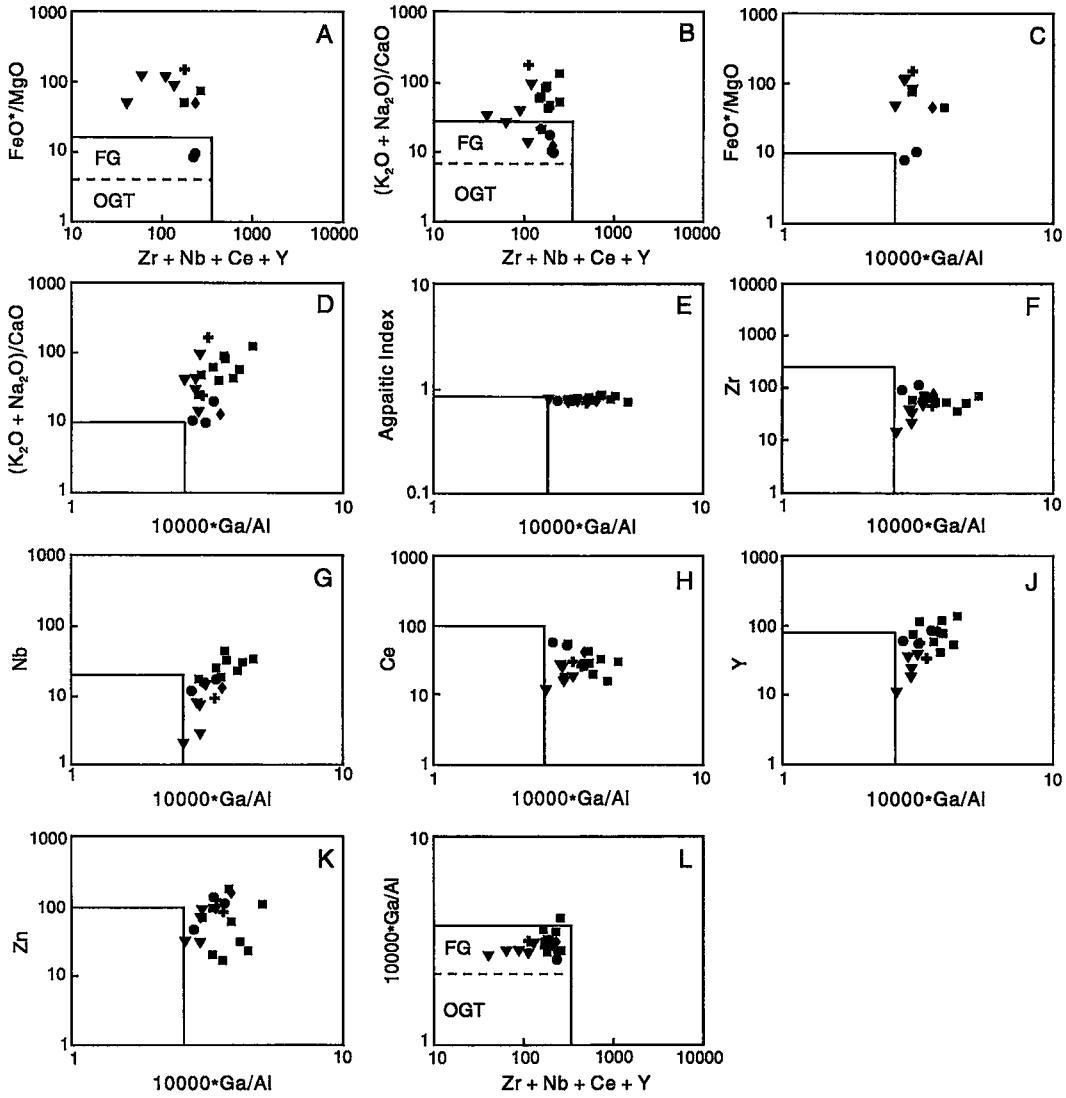

FIG. 8. A. Zr + Nb + Ce + Y *versus* FeO*/MgO discriminant diagram of A-type granites (Whalen *et al.* 1987) (FG, fractionated felsic granites; OGT, unfractionated M-, I- and S-type granites). B. Zr + Nb + Ce + Y *versus* $(K_2O + Na_2O)/CaO$ discriminant diagram of A-type granites (Whalen *et al.* 1987) (FG, fractionated felsic granites; OGT, unfractionated M-, I- and S-type granites. C–L: 10000*Ga/Al *versus* FeO*/MgO, $(K_2O + Na_2O)/CaO$, agpaitic index, Zr, Nb, Ce, Y, Zn discriminant diagram of A-type granites (Whalen *et al.* 1987), and Zr + Nb + Ce + Y *versus* 10000*Ga/Al discriminant diagram of A-type granites (Whalen *et al.* 1987) (FG, fractionated felsic granites; OGT, unfractionated M-, I- and S-type granites). Symbols as for Figure 6A.

CONCLUSIONS

The presence of manganoan-fayalite-bearing granitic pegmatite and of associated fayalite-bearing granitic rocks at Quirra constitutes a new aspect of the regional geology of Sardinia. These pegmatites differ in composition from Sardinian pegmatites so far known (Pani 1994). The high Mn content of the fayalite can be justified by the high silica character of the Quirra leucogranitic magmas from which the pegmatites originated. Watson (1977) experimentally verified that Mn–$K_d^{ol/liq.}$ increases in favor of the olivine as the Si/O atomic ratio of the melt increases.

On the whole, the geochemical character of the leucogranites indicates an origin of a specialized kind, comparable to that of post-orogenic A-type granites of the aluminous trend. The parageneses of the leucogranites from Quirra suggest low-$f(O_2)$ crystallization processes. However, the $f(O_2)$ conditions seem to have changed during the last stages of consolidation of the granite–pegmatite complex, as shown by the low-temperature, subsolidus alteration of the fayalite to laihunite, magnetite, grunerite, greenalite and ferripyrophyllite.

On the basis of geological, mineralogical and geochemical data, the association of quartz + fayalite + microcline + biotite in the Quirra pegmatites is considered to indicate that the pegmatite itself represents a product of crystallization of a residual liquid issued from a parent magma with a composition similar to sample Q11 (Fig. 3, Unit 2), the least-evolved granitic facies in the area. The manganiferous character of the fayalite in the pegmatites, as well as that of some of the host granites, also argues indirectly for the derivation of the pegmatites and the host granites from the same magma.

ACKNOWLEDGEMENTS

Financial support for this work was provided by the Consiglio Nazionale delle Ricerche (E.P. & R.R.), a S.I.M.P. travel award to E.P., and a Natural Sciences and Engineering Research Council of Canada operating grant to MR. We are grateful to R.F. Martin, B. Bonin and an anonymous reviewer for suggestions that substantially improved the manuscript.

REFERENCES

BISTE, M. (1979): Die Anwendung geochemischer Indikatoren auf die Zinn-Höffingkeit herzynischer Granite in Süd-Sardinien. *Berliner geowiss. Abh.* **A18.**

BONIN, B. (1988): Peralkaline granites in Corsica: some petrological and geochemical constraints. *Rend. Soc. It. Mineral. Petrol.* **43**, 281-306.

_____ (1990): From orogenic to anorogenic settings: evolution of granitoid suites after a major orogenesis. *Geol. J.* **25**, 261-270.

BRALIA, A., GHEZZO, C., GUASPARRI, G. & SABATINI, G. (1982): Aspetti genetici del batolite sardo-corso. *Rend. Soc. It. Mineral. Petrol.* **38**, 701-764.

BUDA, G. (1993): Enclaves and fayalite-bearing pegmatitic "nests" in the upper part of the granite intrusion of the Velence Mts., Hungary. *Geol. Sbornik* **44**, 143-153.

CARMIGNANI, L., BARCA, S., CAROSI, R., DI PISA, A., GATTIGLIO, M., MUSUMECI, G., OGGIANO, G. & PERTUSATI, P.C. (1992): Schema dell'evoluzione del basamento sardo. Geologia della Catena Ercinica in Sardegna. *Guida all'Escursione sul basamento paleozoico della Sardegna*, 11-38.

_____, COCOZZA, T., GHEZZO, C., PERTUSATI, P.C. & RICCI, C.A. (1986): Outlines of the Hercynian basement of Sardinia. *In* Guide-book to the Excursion on the Paleozoic basement of Sardinia (L. Carmignani, T. Cocozza, C. Ghezzo, P.C. Pertusati & C.A. Ricci, eds.). *Int. Geol. Correlation Program, Project 5, Newsletter, Special Issue*, 11-21.

CHAPPELL, B.W. & WHITE, A.J.R. (1974): Two contrasting granites types. *Pac. Geol.* **8**, 173-174.

COLLINS, W.J., BEAMS, S.D., WHITE, A.J.R. & CHAPPELL, B.W. (1982): Nature and origin of A-type granites with particular reference to southeastern Australia. *Contrib. Mineral. Petrol.* **80**, 189-200.

DI SIMPLICIO, P., FERRARA, G., GHEZZO, C., GUASPARRI, G., PELLIZZER, R., RICCI, C.A., RITA, F. & SABATINI, G. (1974): Il metamorfismo e il magmatismo paleozoico della Sardegna. *Rend. Soc. It. Mineral. Petrol.* **30**, 979-1068.

EBY, G.N. (1990): The A-type granitoids: a review of their occurrence and chemical characteristics and speculation on their petrogenesis. *Lithos* **26**, 115-134.

_____ (1992): Chemical subdivision of the A-type granitoids: petrogenetic and tectonic implications. *Geology* **20**, 641-644.

EVENSEN, N.M., HAMILTON, P.J. & O'NIONS, R.K. (1978): Rare earth abundances in chondritic meteorites. *Geochim. Cosmochim. Acta* **42**, 1199-1212.

FINGER, F. & STEYRER, H.P. (1990): I-type granitoids as indicators of a late Paleozoic convergent ocean-continent margin along the southern flank of the central European Variscan orogen. *Geology* **18**, 1207-1210.

FROST, B.R., LINDSLEY, D.H. & ANDERSEN, D.J. (1988): Fe–Ti oxide-silicate equilibria: assemblage with fayalitic olivine. *Am. Mineral.* **73**, 727-740.

GHEZZO, C., GUASPARRI, G., RICCOBONO, F., SABATINI, G., PRETTI, S. & URAS, I. (1981): Le mineralizzazioni a molibdeno associate al magmatismo intrusivo ercinico della Sardegna. 1. Rapporti con le plutoniti ed i fenomeni di

alterazione – mineralizzazione. *Rend. Soc. It. Mineral. Petrol.* **38**, 133-145.

_____ & ORSINI J.B. (1982): Lineamenti strutturali e composizionali del batolite ercinico sardo-corso in Sardegna. *Guida alla Geologia del Paleozoico Sardo. Guide Geologiche Regionali. Soc. Geol. It.*, 165-181.

GUASPARRI, G., RICCOBONO, F. & SABATINI, G. (1984a): Leucogranites of Sardinian Batholith: petrologic aspects and their relevance to metallogenesis. *Per. Mineral.* **53**, 17-52.

_____, _____ & _____ (1984b): Hercynian Mo-mineralizations of porphyry-style in the Sardinian Batholith: a discussion on the genesis and a comparison with other deposits of the family. *Rend. Soc. It. Mineral. Petrol.* **39**, 629-648.

HIRT, W.H. (1991): Development of fayalite-bearing pegmatites during late-stage crystallization of the Sawtooth Batholith, central Idaho. *Geol. Soc. Am., Abstr. Program* **23**, A328.

JANECZEK, J. (1989): Manganoan fayalite and products of its alteration from the Strzegom pegmatites, Poland. *Mineral. Mag.* **53**, 315-325.

LOISELLE, M.C. & WONES, D.R. (1979): Characteristics and origin of anorogenic granites. *Geol. Soc. Am., Abstr. Program* **11**, 468.

LOVISATO, D. (1900): Fayalite alterata delle granuliti di Villacidro. *Rend. R. Acc. Naz. Lincei* **60**, 10-13.

MANIAR, P.D. & PICCOLI, P.M. (1989): Tectonic discrimination of granitoids. *Geol. Soc. Am., Bull.* **101**, 635-643.

MIDDLEMOST, E.A.K. (1994): Naming materials in the magma/igneous rock systems. *Earth Sci. Rev.* **37**, 215-224.

MILLS, J.G., JR. & ROSE, T.P. (1991): Manganoan fayalite [$(Fe,Mn)_2SiO_4$]: a new occurrence in rhyolitic ash-flow tuff, southwestern Nevada, U.S.A. *Am. Mineral.* **76**, 288-292.

MORRA, V., SECCHI, F.A. & ASSORGIA, A. (1994): Petrogenetic significance of peralkaline rocks from Cenozoic calc-alkaline volcanism from SW Sardinia, Italy. *Chem. Geol.* **118**, 109-142.

PALACHE, C. (1950): Fayalite at Rockport, Massachusetts. *Am. Mineral.* **35**, 877-881.

PANI, E. (1994): *I tipi delle pegmatiti associate al Batolite Sardo: studio, caratterizzazione e classificazione.* Ph.D. thesis, Univ. of Cagliari, Cagliari, Italy.

_____, RIZZO, R. & RAUDSEPP, M. (1994): Hydrothermally altered manganoan fayalite in the Rio Forrus pegmatite, Quirra, southeast Sardinia. *Geol. Soc. Am., Abstr. Program* **26**, A357.

PEARCE, J.A., HARRIS, N.B.W. & TINDLE, A.G. (1984): Trace element discrimination diagrams for the tectonic interpretation of granitic rocks. *J. Petrol.* **25**, 956-983.

PITCHER, W.S. (1979): Comments on the geological environments of granites. *In* Origin of Granite Batholiths: Geochemical Evidence (M.P. Atherton & J.Tarney, eds.). Shiva Publ., Ltd., Orpington, Kent, 1-8.

PONCE, P.F., PINGITORE, N.E., JR., HOFFER, J.M., ANTHONY, E.Y. & WORONOW, A. (1993): Discrimination of topaz rhyolite by major-element composition: a statistical routine for geochemical exploration. *J. Geochem. Explor.* **49**, 269-285.

POUCHOU, J.L. & PICHOIR, F. (1985): PAP $\varphi(\rho Z)$ procedure for improved quantitative microanalysis. *Microbeam Analysis* **1985**, 104-106.

RIZZO, R., PANI, E. & RAUDSEPP, M. (1996): Rare-element mineralogy of granitoids associated with fayalite-bearing pegmatites, Quirra, southeast Sardinia. *Geol. Assoc. Can. – Mineral. Assoc. Can., Program Abstr.* **21**, A79.

SCHAEFER, M.W. (1983): Measurements of iron(III)-rich fayalites. *Nature* **303**, 325-327.

_____ (1985): Site occupancy and two-phase character of "ferrifayalite." *Am. Mineral.* **70**, 729-736.

SUN, SHEN-SU (1982): Chemical composition and origin of the Earth's primitive mantle. *Geochim. Cosmochim. Acta* **46**, 179-192.

WATSON, E.B. (1977): Partitioning of manganese between forsterite and silicate liquid. *Geochim. Cosmochim. Acta* **41**, 1363-1374.

WHALEN, J.B., CURRIE, K.L. & CHAPPELL, B.W. (1987): A-type granites: geochemical characteristics, discrimination and petrogenesis. *Contrib. Mineral. Petrol.* **95**, 407-419.

Received April 26, 1996, revised manuscript accepted December 17, 1996.